TIME RESOLVED OPTICAL DETECTION OF ELECTRON LOSS AND MIGRATION IN CdS

G. Chang, R.B. Givens, J.W.M. Spicer, and J. C. Murphy

The Johns Hopkins University
Applied Physics Laboratory
Johns Hopkins Road, Laurel, MD 20723-6099

INTRODUCTION

A beam of energetic electrons incident on a semiconductor produces a variety of effects depending on the primary beam energy and on the properties of the semiconductor. These effects include electron penetration, internal ionization and thermal deposition as well as external effects such as secondary and back scattered electrons, electron beam induced current (EBIC) and lattice strain. Modulated electron beams have been used for thermal wave imaging by the use of piezoelectric detectors in contact with the sample to monitor the modulated strain produced by the electron beam. This technique is termed Scanning Electron Acoustic Microscopy (SEAM). SEAM studies of integrated circuits have shown that subsurface features are imaged at depths controlled by the energy of the electron beam [1]. However, there is no adequate theory which describes this effect or the more general question of image contrast in SEAM. This arises in part because SEAM images represent a convolution of thermal, acoustic and electron transport effects as well as the initial electron loss profile in the semiconductor. There is a need for improved understanding of electron injection, scattering, trapping and thermalization especially as they apply to the use of electron excitation beams for thermal wave imaging.

This paper presents Optical Beam Deflection (OBD) studies of CdS using an electron beam as an excitation source and a subbandgap optical beam as a probe to study electron transport mechanisms resulting from electron loss in the specimen. The OBD method monitors the deflection of the probe beam produced by an index of refraction gradient field in the sample induced by the exciting beam [2, 3]. Beam deflection measurements were made as a function of depth in both the time and frequency domains. In principle extensions of this method should permit *in situ* monitoring of the range of primary electrons as well as the determination of the rates of electron trapping and thermalization.

Earlier OBD studies in semiconductors have used a laser beam as the excitation source and have shown that both thermal and electron density gradients are sources for the index gradient field. These gradients have been shown to occur both by direct excitation and by diffusion [4]. In earlier work we have used modulated electron beams of varying energy and have shown that both mechanisms contribute to the observed beam deflection [5, 6]. In the present work the contributions of the thermal and electronic mechanisms are resolved in the time domain. Since the electron beam interaction with the specimen differs from the laser case, the effects of electron range, scattering, internal ionization and trapping must be considered. In addition, an improved analytical model is required to represent the OBD signal generation process. The prior studies made using a laser source all assumed that the optical energy was absorbed at the surface of the specimen and that variations in the index field at interior points in the specimen

Review of Progress in Quantitative Nondestructive Evaluation, Vol. 10B
Edited by D.O. Thompson and D.E. Chimenti, Plenum Press, New York, 1991

occurred solely by electron and thermal diffusion with no component of direct excitation. This model is inadequate for the present studies because of the combined effects of volume excitation by the penetrating electron beam and due to the effects of electron trapping and delayed thermalization. Development of a more complete analytical model which includes the effects of volume excitation and electron diffusion and thermalization is in progress.

THEORY

Consider the specimen temperature on epicenter (directly below the point of entry of the electron beam normally incident on the top face of the specimen) at a depth, z, below the sample surface. In this development no direct electron excitation is assumed and the region which is directly excited by the incident electrons can be represented as a small spherical source located near the surface of the sample. The temperature, T(z, t), can be calculated using an approximate three-dimensional thermal diffusion analysis as:

$$T(z, t) = \frac{Q}{8(\pi\alpha t)^{3/2}} \exp\left(-\frac{\tau_z}{t}\right) \qquad [1]$$

where

$$\tau_z = \frac{z^2}{4\alpha} \quad . \qquad [2]$$

T(z, t) has the functional form illustrated in Fig. 1 with the time of the peak, t_p given by

$$t_p = \frac{2}{3}\tau_z \quad . \qquad [3]$$

In these expressions Q denotes the heat energy, z the depth of the probe beam in the specimen and α the thermal diffusivity. The expression for the peak temperature will be compared later with experimental data.

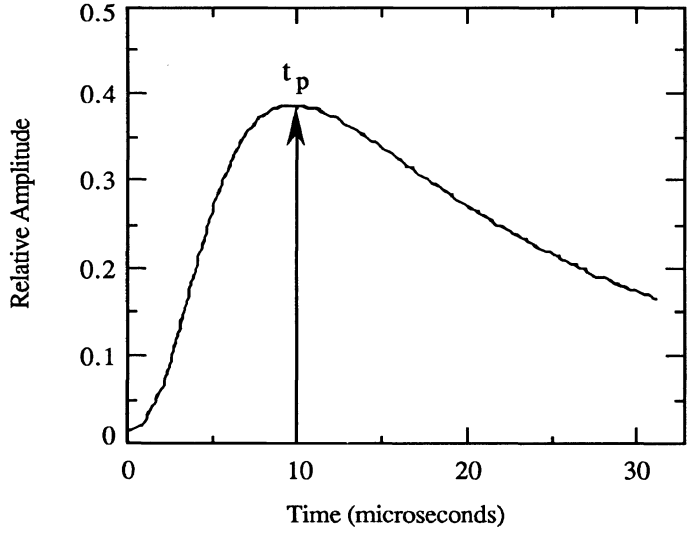

Fig. 1. Theoretical plot showing dependence of specimen temperature at depth, z, as a function of time. The time at which the peak temperature occurs is denoted by t_p.

Gradients in the electron density also can contribute to the observed index gradient field inside the sample and hence to the beam deflection. The normal component of the index of refraction field in a semiconductor can be written formally as:

$$\frac{dn(T_{1,2}, N_{1,2})}{dz} = \frac{\partial n}{\partial T_1}\frac{dT_1}{dz} + \frac{\partial n}{\partial T_2}\frac{dT_2}{dz} + \frac{\partial n}{\partial N_1}\frac{dN_1}{dz} + \frac{\partial n}{\partial N_2}\frac{dN_2}{dz} \qquad [4]$$

The first and second terms on the right hand side describe the index gradient due to the temperature field (T_1) due to thermal diffusion and the temperature field (T_2) due to thermalization of diffused electrons. The third and fourth terms are determined by the gradient in the electron density. The two contributions to the electron density are direct electron injection including the effects of scattering (N_1) and electron diffusion (N_2). In semiconductors deflections due to electron density effects are of opposite sign than deflections due to thermal effects. The temperature distribution calculated in Eq. 1 is used to provide the temperature gradient, $\partial T_1/\partial z$ for Eq. 4.

EXPERIMENTAL

The experimental configuration is shown in Fig. 2. A focused, amplitude-modulated electron beam of energy, E (2.5 keV < E < 30 keV) is produced in a modified commercial scanning electron microscope (SEM). This instrument can produce 10 nanosecond, 80 microampere pulses. The electron beam is incident on a thin edge of an optically clear CdS plate of thickness d = 35 μm. The position of the electron beam was either fixed at one point on the sample or rastered along the top of the specimen. A helium-neon probe beam was focused inside the specimen with the probe beam waist , w = 15 μm. The probe beam deflection was measured using a position sensitive detector and associated electronics which had a bandwidth of 20 MHz. The depth of the probe beam below the sample surface was also controlled. Probe beam deflection was measured as a function of probe beam depth, offset from the center of the electron beam and electron beam energy in both CW and time domain regimes.

RESULTS AND DISCUSSION

Figure 3 shows the time development of the normal component of the probe beam deflection for a depth 35 μm below the surface illuminated by the electron pump beam. The two vertical lines in the figure indicate the duration of the pump beam. The first feature, A, is a small, fast, negative deflection followed immediately by a positive-going signal, B. Still later is a much larger positive-going signal, C. The peak time for feature C, t_p, was measured as a function of probe beam depth, z. This time is plotted versus z^2 in Fig. 4 and shows a linear dependence. This indicates that peak C is due to a diffusion process in the sample and using Eqs. 2 and 3, a value for the diffusion coefficient of 0.11 cm^2/sec is obtained. This value is in good agreement with literature values for the thermal diffusivity, α, in CdS which range from 0.098 - 0.12 cm^2/sec. We conclude that feature C corresponds to thermal diffusion from near-surface heating.

Feature A occurs at shorter times than feature C. Moreover, for electron pump times longer than approximately 100 nsec, the width of feature A is constant for probe beam positions close to the specimen surface. This indicates that feature A is an electronic effect due to the ionization and penetration of electrons. The structure of feature A is complex and changes shape as a function of probe beam depth and electron beam energy.

Figure 5 shows the normal component of the optical beam deflection for 3 probe beam depths in the sample. The onset of feature A is coincident with the pump onset and both its width and the time of its peak increase with increasing depth. The amplitude of feature A depends on electron beam energy as shown in Fig. 6 for a probe beam depth of 6 μm. The magnitude of feature A decreases as the beam energy is decreased from 30 keV through 5 keV. Additional work is in progress to investigate the near surface region in greater detail in order to

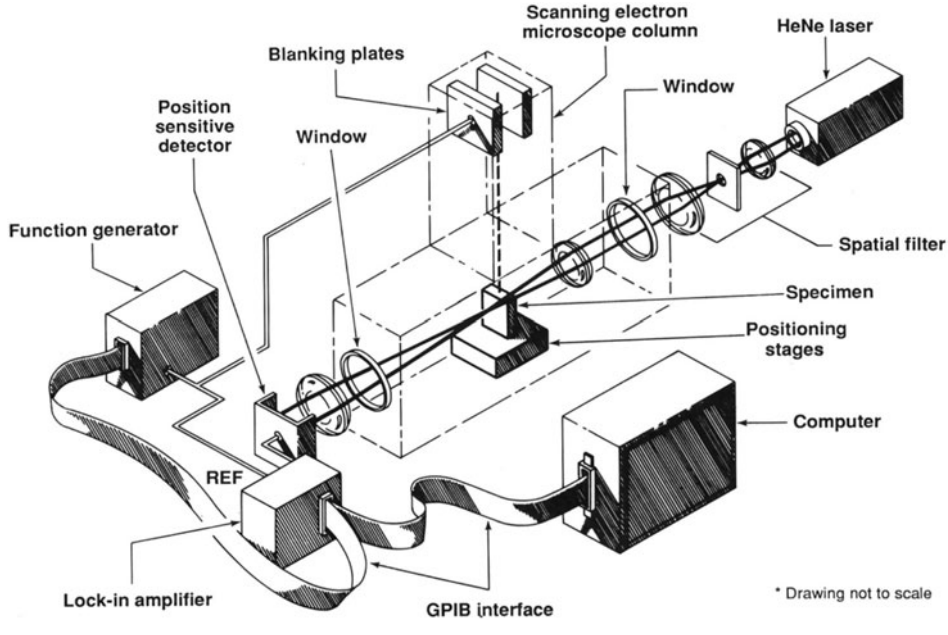

Fig. 2 Block diagram of the modified scanning electron microscope used in the SEM/OBD experiments. The probe beam passes through the CdS specimen and its deflection is measured by the position sensitive detector . For time domain measurements, the function generator is replaced with a pulse generator.

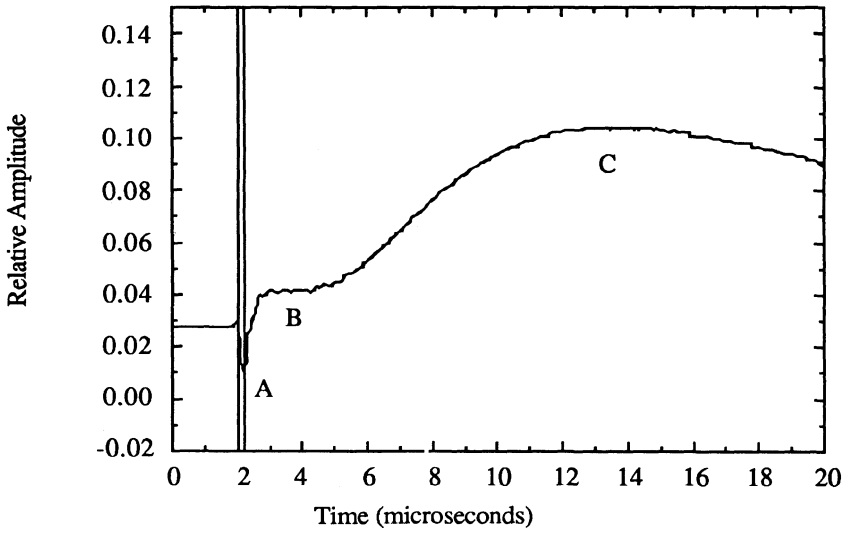

Fig. 3 Time-resolved normal component of the optical beam deflection for a probe beam depth of 35 μm. The negative and subsequent positive deflection peaks are associated with electronic effects and thermal diffusion respectively.

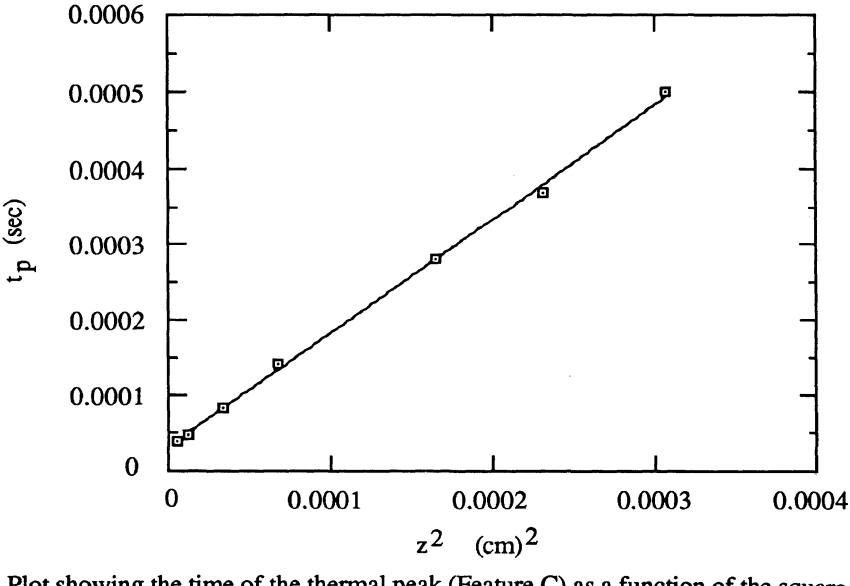

Fig. 4 Plot showing the time of the thermal peak (Feature C) as a function of the square of the probe beam depth. The value of thermal diffusivity calculated from the slope of this graph is 0.11 cm^2/sec.

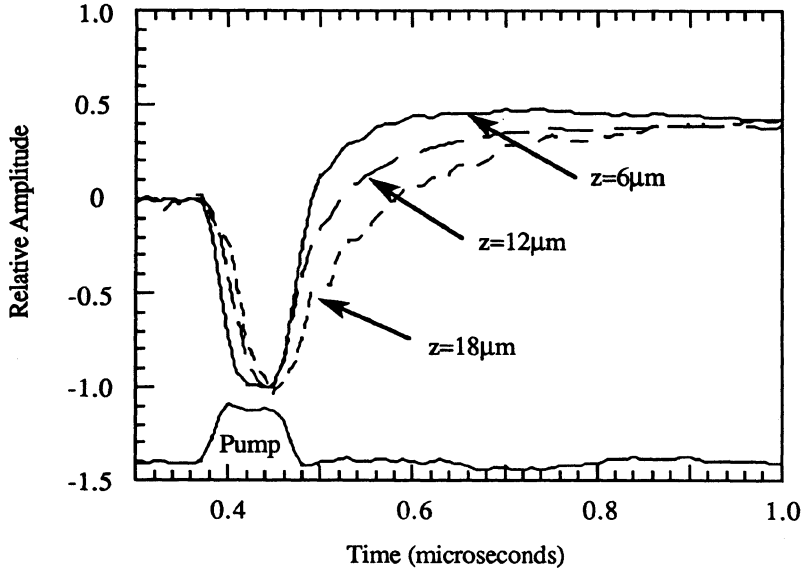

Fig. 5 Normal component of the optical beam deflection for 3 probe beam depths showing the development of feature A as a function of depth. The bottom trace shows the time and duration of the electron beam pulse obtained with a Faraday cup in the specimen chamber.

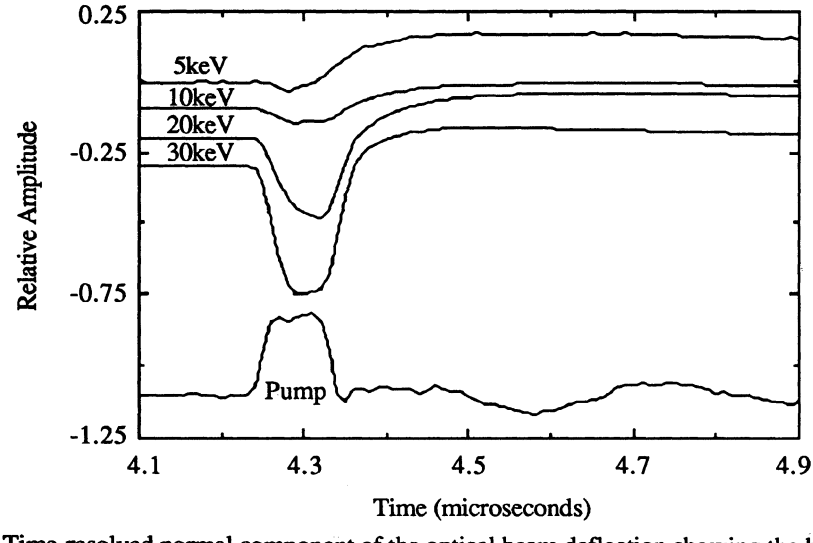

Fig. 6 Time-resolved normal component of the optical beam deflection showing the behavior of the electronic peak as a function of electron beam energy.

distinguish possible effects associated with direct electron injection from those tied to elastic and inelastic scattering.

Feature B, the positive-going signal observed at short times for probe positions close to the surface, has the same sign as the later arriving thermal diffusion wave (feature C). This result suggests that feature B is associated with the thermalization of diffused or diffusing electrons possibly delayed by electron trapping and subsequent thermalization.

CONCLUSIONS

Optical beam deflection measurements have been used to monitor electron injection and thermalization in CdS. Time-resolved measurements of the deflection of a subbandgap probe beam shows several components which can be associated with electron injection, thermalization and thermal diffusion. The depth dependence of the thermal diffusion component yields values for the thermal diffusivity which agree well with literature values. While no detailed model of the electron injection and thermalization process is presented in this work, we believe that such a model can be developed and will yield fundamental information about electron injection and transport mechanisms in the near surface region of semiconductors. Information of this kind is important for improved understanding of image formation and contrast in SEM and SEAM imaging as well as improved knowledge of electron beam lithography.

REFERENCES

1. J.C. Murphy, J.W. Maclachlan and L.C. Aamodt, IEEE Trans. Ultrason., Ferroelec. and Freq. Contr., Vol. UFFC-33, No. 5, p. 529 (1986).
2. A.C. Boccara, D. Fournier and J. Badoz, Appl. Phys. Lett, Vol. 36, p. 136, 1980.
3. J.C. Murphy and L.C. Aamodt, J. Appl. Phys., Vol. 52, p. 196 (1981).
4. D. Fournier, A.C. Boccara, A. Skumanich and N.M. Amer, J. Appl. Phys., Vol. 59, p. 787 (1986).
5. J.W. Maclachlan, J.C. Murphy and L.C. Aamodt, Bull. Am. Phys. Soc., Vol. 33, p. 301 (1988).
6. J.C. Murphy, J.W. Maclachlan Spicer, R.B. Givens, L.C. Aamodt and G. Chang, in Photoacoustic and Photothermal Phenomena, J.C. Murphy, J.W. Maclachlan Spicer, L.C. Aamodt, B.S.H. Royce, eds., Springer Series in Optical Sciences (Springer-Verlag, Berlin, Heidelberg, 1990) p. 249.